Modern Ocean Current-Controlled Sediment Transport in the Greenland-Iceland-Norwegian (GIN) Seas

Hermann Fohrmann[1], Jan O. Backhaus[2], Frank Blaume[1], Bernd J. Haupt[1], Jochen Kämpf[2], Klaus Michels[3], Jürgen Mienert[4], Jörg Posewang[1], Will Ritzrau[1], Jan Rumohr[5], Mathias Weber[1] and Rebecca Woodgate[3]

[1] SFB 313, Kiel University, Heinrich-Hecht-Platz 10, 24118 Kiel, Germany
[2] Institute of Marine Science, Hamburg University, Troplowitzstrasse 7, 22529 Hamburg, Germany
[3] Alfred Wegener Institute for Polar and Marine Research, Columbusstrasse, 27568 Bremerhaven, Germany
[4] Institute of Geology, University of Tromsø, Dramsveien 201, 9037 Tromsø, Norway
[5] GEOMAR, Research Center for Marine Geosciences, Kiel University, Wischhofstrasse 1–3, 24148 Kiel, Germany

Abstract: Sediment transport processes in the northern North Atlantic have been investigated on the basis of various numerical models. A general circulation model has been used to investigate large-scale particle transport, a reduced gravity plume model has been used to investigate particle transport by cascading from the shelves into the deep basins, an ocean slice model has been used to investigate particle exchange processes between a bottom current and the ambient water mass, and a Bottom Boundary Layer model has been used to investigate particle interactions influencing the settling behavior of suspended particles. In this paper, the various processes investigated in these models are described (i) schematically, (ii) on the basis of field data, if available, and (iii) by employing results from numerical simulations. In a first attempt the northern North Atlantic will be divided into separate process defined areas, which can be used in carbon budgeting, for example.

Introduction

Generally, marine sediment transport is strongly coupled to ocean circulation and sediment supply. If the settling velocity of the particles is small enough, the rain of particles sinking through a 'water column' from the surface layer to the ocean floor is spread over entire ocean basins. For example, the regime of the surface currents in the Greenland-Iceland-Norwegian Seas, as shown in Figure 1 (Poulain 1996), illustrates that particles released at any certain location can statistically be deposited anywhere in the Greenland-Iceland-Norwegian Seas, and that a noticeable meridional exchange of particles takes place (Haupt et al. 1994, 1998). Large-scale particle transport through the general circulation regime is modified in time and space by small-scale transport processes from shallow shelves or the continental slope to the deep basins, which, in turn, are controlled by local hydrographic and topographic environments (Fohrmann et al. 1998). The fact that as much as 83 % of marine organic carbon burial occurs in continental slope sediments (Berner 1982) indicates that cross-slope transport processes are crucial for estimating particle transport budget. In this context, the most active processes for particle erosion or transport are (i) cascading of particle-laden dense bottom-water masses ('turbidity plumes'), (ii) interactions of turbulent eddies with the seafloor, and (iii) erosion due to the surf of internal waves. These processes are closely coupled to topography, because dense bottom-water masses tend to flow to the deepest sites and to follow steepest slopes. Cascading takes place in troughs below topographic cuts at the shelf edge. Eddy-seafloor interactions may take place within Taylor columns above deep-sea mountains. The surf of internal waves is largest where the inclination of the slope equals the propagation angle of the waves.

The present paper is divided into three parts. First, simulation results of large-scale particle transport in the northern North Atlantic will be presented. Following

From *The Northern North Atlantic: A Changing Environment*, edited by P. Schäfer, W. Ritzrau, M. Schlüter, and J. Thiede, pp. 135–154, Springer, Berlin, 2000

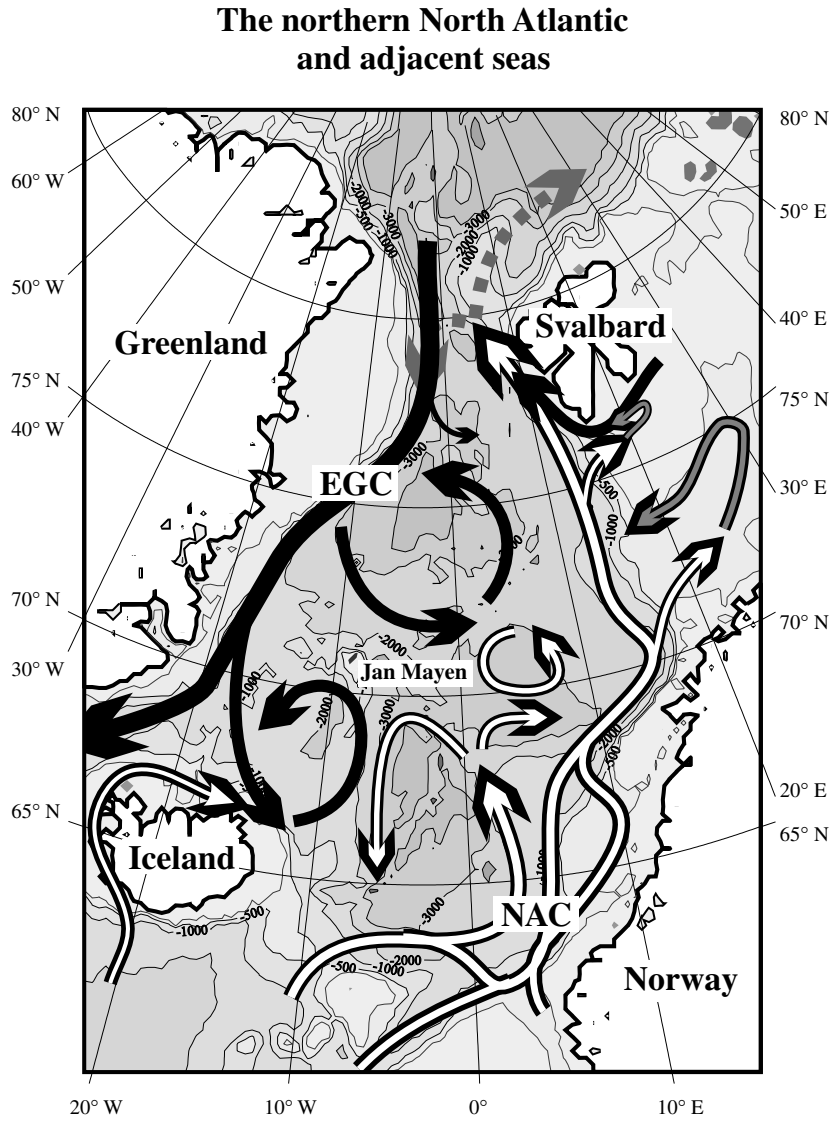

Fig. 1: Topography of the northern North Atlantic (Greenland-Iceland-Norwegian Seas) including current regime modified after Poulain (1996). White: warm and saline Atlantic Water; Black: cold and less saline Polar Water

that, the various above-mentioned small-scale processes which modify particle transport will be discussed. Then the physical conditions and background which are essential for gaining a deeper understanding of these processes will be described. Subsequently, field data, where available, and numerical simulation results will be presented. Large-scale particle transport in paleoenvironments will be discussed in the following section by identifying current transported sediment fractions and reconstructing critical shear velocities as well as maximum geostrophic current velocities for their transport. Based on the regional distribution of steep slopes, a first attempt to divide the northern North Atlantic into areas in which various processes dominate will be presented in the final section. Such a division may then be used for future budgeting attempts.

Much scientific work has been conducted into the hydrography of the Greenland-Iceland-Norwegian Seas. A detailed review has been written by Hopkins (1988). The physiographic setting of the Greenland-Iceland-Norwegian Seas has been nicely described by Vogt (1986) and Vorren et al. (1998). The introductory article by Schäfer et al. in this volume summarizes the latest literature.

Large-Scale Particle Transport

Simulations of large-scale particle transport are based on the general circulation system of the North Atlantic or the global ocean. In the approach taken here, traditional simulations of ocean circulation were combined using an Ocean General Circulation Model (OGCM), a sediment transport model, and a semi-Lagrangian trajectory-tracing technique. The current velocities calculated by (i) an intermediate planetary-geostrophic model for the North Atlantic (Seidov 1986, 1996) and (ii) a global OGCM (Bryan 1969; Cox 1984; Pacanowski et al. 1993; Seidov and Haupt 1997b) are used by the trajectory-tracing model (Haupt et al. 1994; Seidov and Haupt 1997a; Haupt et al. 1998). Every set of these models has a different horizontal and vertical resolution, and is either global or local. The global set has a coarse resolution (6° longitude by 4° latitude) to facilitate multiple long-term runs (Seidov and Haupt 1997b), whereas the more regional study of the North Atlantic has a $2° \times 2°$ horizontal resolution (Seidov and Haupt 1997a). In both cases, the vertical extension is divided into twelve unevenly spaced levels (see Fig. 2). To calculate sediment transport an additional 1-cm-thick bottom layer is introduced to the regional model.

One selected result of the model runs demonstrates that slow settling particles (w_s = 0.00015 cm s^{-1} ~ 1.3 cm day^{-1}, a typical value for bacteria chosen as the lower limit for settling velocities) released in the Greenland-Iceland-Norwegian Seas are redistributed over the entire basin. Furthermore, they can escape from the Greenland-Iceland-Norwegian Seas to the North Atlantic (Fig. 2a), and eventually farther on to the South Atlantic (Fig. 2b). This is in good agreement with large sediment drifts, as described by Haupt et al. (1998).

The sediment transport model is used to calculate sediment transport through specified gateways or cross-sections, e.g. the Denmark Strait, the Iceland-Faeroe-Scotland-Ridge, or Barents Sea inflow and outflow (Fig. 3). Here, the outflow of particles from coastal sources as well as the inputs of Aeolian dust (0.0864 mg m^{-2} d^{-1}) and melting icebergs have been prescribed as sediment sources. A detailed description is given by Haupt et al. (1994, 1998).

Small-Scale Particle Transport

Sedimentation rates and the fraction of terrigenous matter in sediments on continental slopes are higher than in the center of deep basins (Vogt 1986; Vorren et al. 1998). Up to 83 % of marine organic carbon burial occurs in continental slope sediments (Berner 1982). Turbidites are a common feature in sediment cores in the northern North Atlantic. Along the continental slopes of the Greenland-Iceland-Norwegian Seas seven Trough Mouth Fans (TMF) have been detected, which were formed by slides, debris flows and turbidity currents (Vorren et al. 1998; Laberg and Vorren 1995). The latter two processes have formed several gullies and channels along the continental margins, which may potentially be used by modern turbidity plumes.

All these indicate that deep-sea sediments are essentially influenced by lateral transport processes of various intensity and magnitude. Lateral transport processes at the continental margin are strongly coupled to small-scale bottom topography and are, therefore, of a much smaller scale than particle transport by large-scale geostrophic currents. Some of these processes – cascading, Taylor columns, internal waves – and particle interactions which influence settling velocity are described in the following sections. A schematic overview of the processes influencing sedimentation is given first, followed by descriptions of measurements and the results of numerical simulations.

Schematic Process Description

Cascading

Dense bottom-water masses are produced on shallow shelves during winter (Fig. 4) (Killworth 1983; Aagaard et al. 1985). The density of water increases due to cooling and salt brine is released as a result of salt water freezing (Rudels et al. 1991). Following bottom topography, the newly formed bottom water flows as a gravity plume to the shelf edge and cascades down the continental slope (Quadfasel et al. 1988; Aagaard 1989; Jungclaus et al. 1995; Schauer 1995). On the way down, the ambient water masses are entrained. Eventually, the plume reaches its depth of equilibrium density and either penetrates the ambient ocean water or travels along the continental slope as a contour current (Backhaus et al. 1997). The dynamics and the structure of those plumes may be altered completely if they reach areas with erodible sediments at the seafloor and if the velocity of the flow is high enough to resuspend particles. With higher density contrasts, due to the additional sediment load, the sediment-laden turbidity plumes descend faster and deeper into deep-ocean basins (Fohrmann et al. 1998).

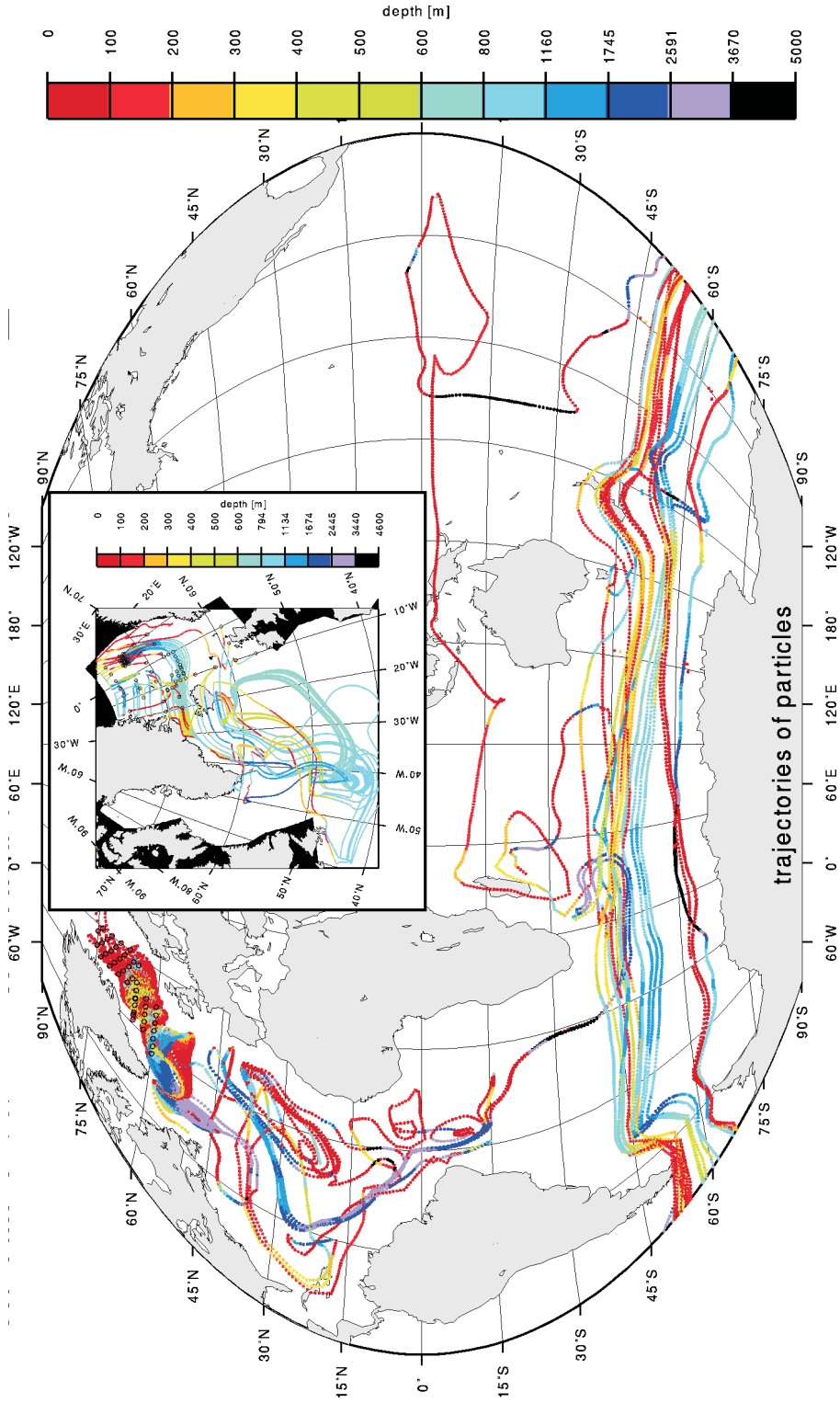

Fig. 2: Trajectories of Lagrangian particles begun in the upper 200 meters (global experiment) or 100–2000 meters (North Atlantic experiment) of the water column. Small circles show the location at which the particles were launched. The global experiment was run over 1000 years, whereas the regional North Atlantic experiment was run over 500 years. Both experiments show particle export from the Greenland-Iceland-Norwegian Seas into the North Atlantic as well as their connection to the global ocean

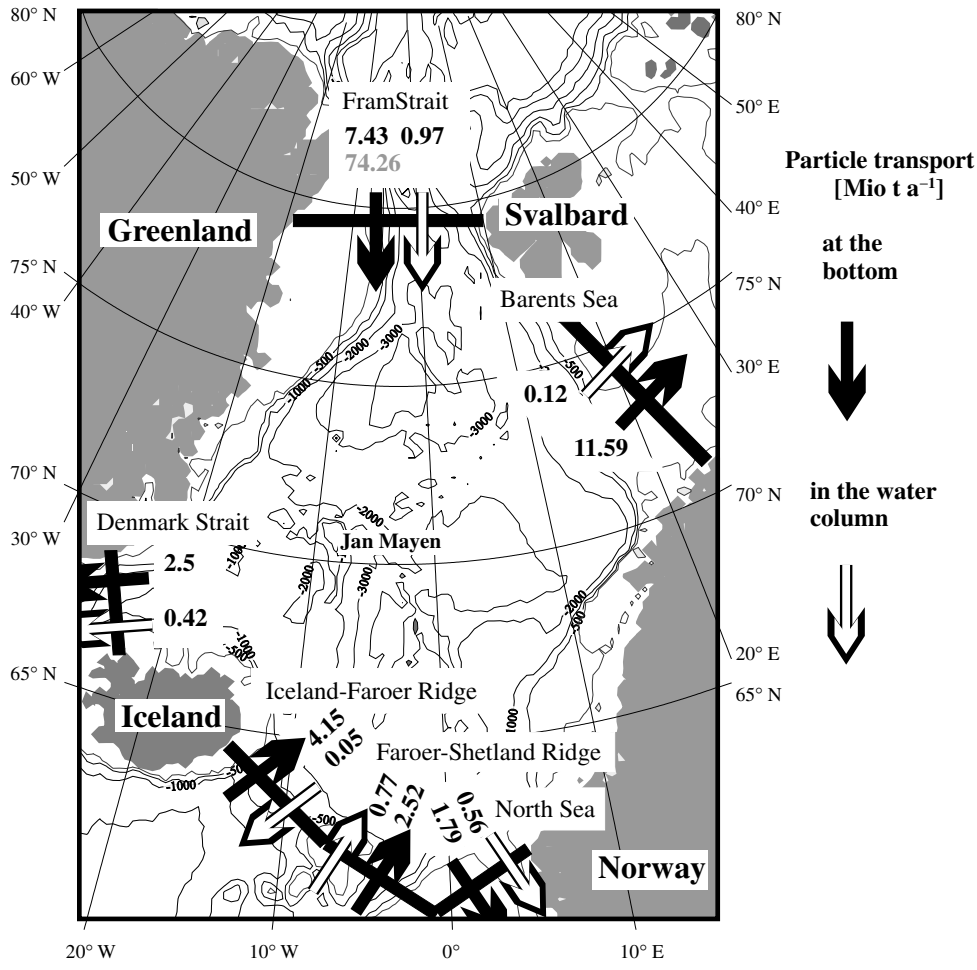

Fig. 3: Calculated sediment transport rates for the three-dimensional water column and for the bottom layer through specified gateways (Haupt et al. 1998). The bottom layer is 1 cm thick

Taylor Columns

In a homogeneous ocean without friction, potential vorticity (Π) defined as a sum of planetary vorticity (f), which is constant at a given latitude, and relative vorticity (ξ) divided by depth (h), is a conservative quantity (Pedlovsky 1987):

$$\Pi = (f + \xi) / h = \text{const.} \qquad (1)$$

As Equation 1 suggests, a reduction in depth (h) reduces relative vorticity. Negative relative vorticity means clockwise rotation, whereas positive relative vorticity means counterclockwise rotation. Reducing relative vorticity is equivalent to adding negative vorticity and induces an anticyclonic (clockwise) vortex. Figure 5 illustrates the vorticity conservation principle.

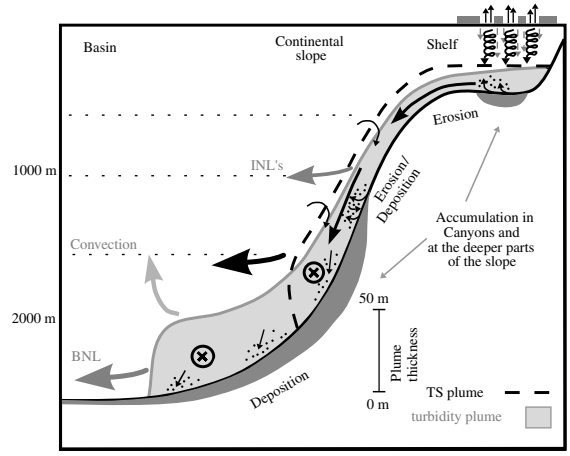

Fig. 4: Cascading of dense bottom-water masses. (TS plumes are temperature and salinity plumes, circles with cross symbols indicate flow into the figure)

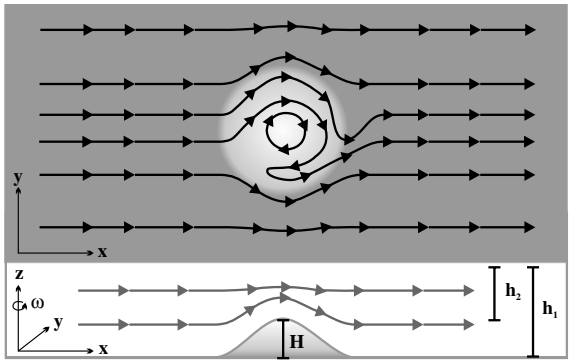

Fig. 5: Idealized Taylor column. Below: A flow streaming towards a rise in the seafloor. The water column is compressed above and stretched again behind the rise. Above: The resulting negative relative vorticity (see text for details) induces an anticyclonic vortex (modified after Ross 1991)

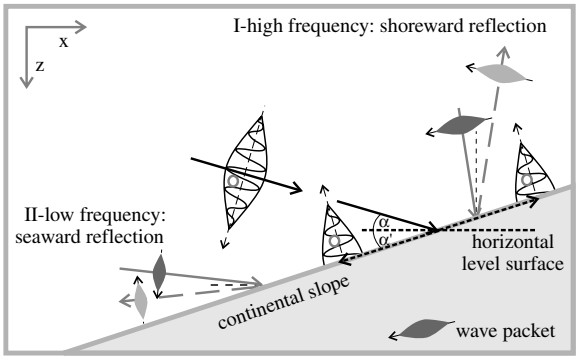

Fig. 6: Internal wave reflection. I: relatively high frequency (w >> N); II: relatively low frequency (w >> f); III: critical reflection if the angle of propagation is equal to the inclination of the slope (for details see text; modified after LeBlond and Mysak 1978 and Munk 1981)

Whenever a current flows over a rise in the seafloor, e.g. a deep-sea mountain or a plateau, the water column contracts ($h_2 = h_1 - H$). This decrease in water column thickness leads to a relative vorticity decrease (or an addition of negative relative vorticity), speeding up clockwise rotation. Behind the rise, the water column is stretched again, and flow turns back. Depending on flow velocity and the size of the rise, the anticyclonic vortex above the rise can be shifted downstream and may be superimposed by the current regime. Due to low flow velocities in the center of the vortex, particles can be trapped and deposited, as described below.

Internal Waves

In stratified fluids, internal waves are three-dimensional (LeBlond and Mysak 1978; Munk 1981). The propagation angle (α between wave direction and the horizontal plane) depends on the frequency of the internal wave (ω), on the stability of stratification N (the Brunt-Väisälä-Frequency), and on the inertial frequency (f). The last components are the upper and lower limits for frequencies at which internal waves may occur ($f < \omega < N$). Internal waves propagate more horizontally if their frequency is relatively low ($f < \omega << N$) and more vertically if their frequency is relatively high ($f << \omega < N$). In a discontinuously stratified ocean, stability varies with depth ($N = N(z)$). Density stratification is often weak at the surface and in deeper layers due to mixing. Here, the Brunt-Väisälä-Frequency may fall below the frequency of the internal wave; the wave is reflected if N equals ω. The internal wave is trapped in a depth interval where N(z) is greater than ω. Thus, the stratification of the ocean defines depth intervals in which internal waves may reach the continental slope. If they do so, they are reflected "shoreward" (Fig. 6.I) or "seaward" (Fig. 6.II). Propagation direction depends only on frequency, stability, and inertia, which are conservative at the point of reflection. Therefore, incident and reflected angles are symmetric in relation to a level surface rather than in relation to the reflecting surface. In a critical case in which the propagation angle of the waves equals the inclination of the slope, internal waves can be reflected parallel to the seafloor, with orbital flow also parallel to the seafloor. Thus, high flow velocities and sediment erosion can be induced by internal waves at distinct depth intervals (Huthnance 1995; Thorpe and White 1988; Fahrbach and Meincke 1982). This, and winnowing by the Norwegian Current (Kenyon 1986), explains why lag sediments have often been found at the shelf edge (Elverhøi and Solheim 1983; Pfirman 1985).

Particle Interaction in the Bottom Boundary Layer

Particles in the Bottom Boundary Layer (BBL) differ in quantity and composition from particles in the euphotic zone or in the intermediate water column (McCave 1984). A conceptual model (Fig. 7) describes the dynamics of aggregates in the vicinity of the seafloor (Ritzrau and Fohrmann 1998). Large aggregates settling in the BBL can be destroyed (disaggregation) if the Kolmogoroff length (the typical length scale of turbulent eddies) is smaller than the aggregate diameter. The smaller fractions of the aggregate may be transported upward again (turbulent diffusion). At higher, more tranquil elevations particles may accu-

mulate, thus forming larger aggregates which consequently begin to settle again. Thus, hydrodynamic sorting, in terms of particle diameter, produces characteristic particle distributions in the BBL.

These interactions influence sediment transport in two varying ways. Above the BBL settling velocities may be enhanced, frequently observed marine snow settles with settling velocities of up to 200 m d^{-1} (~ 0.23 cm s^{-1}; Alldredge and Silver 1988). In the BBL the effect is more complex. Rapidly sinking particles are destroyed and redistributed. Therefore the residence time and transport distance of particles in the BBL is prolonged as compared to calculations based on settling velocity alone.

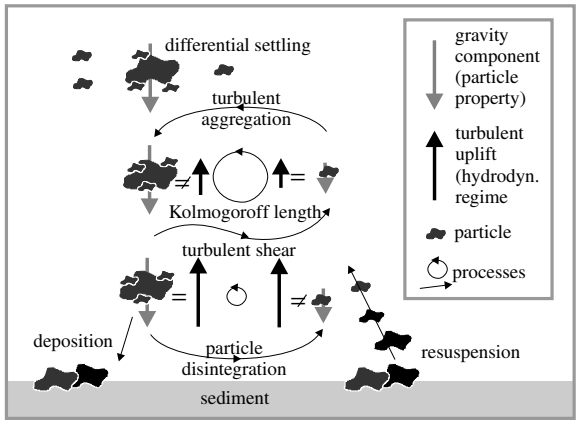

Fig. 7: Theoretical model of particle dynamics close to the seafloor including settling, aggregation, disaggregation and resuspension (Ritzrau and Fohrmann 1998)

Modeling and Measurements

Cascading / Turbidity Plumes

A site which is not influenced by terrigenous particle input by rivers or glaciers would be most suitable for the investigation of cascading by turbidity plumes. The Kveitehola Valley (75° N, 17° E) north of Bear Island functions as a drainage system for dense bottom-water masses (Fohrmann 1996; Fohrmann et al. 1998 and references therein; cf. also references in sections above). Leaving the shallow Spitsbergen Banken bottom-water masses flow via the Kveitehola Valley into the deep Norwegian Sea. On its way, water flow erodes particles from the ocean floor and transports them into the deep sea. The resulting high-accumulation area at the base of the continental margin has been revisited and studied during numerous expeditions since 1988. 3.5-kHz echo sounder profiles, sediment cores and oceanographic measurements aid in understanding sediment texture and the oceanographic environment above the high-accumulation area as well as on the potential pathway to the source areas at Spitsbergen Banken.

Generally, the input of sediments from other areas to the study area is possible, but difficult to quantify. For example, sediments can be eroded farther south, e.g. at the Bear Island Trough Mouth Fan, or they can be transported by other turbidites, e.g. through the INBIS channel. The effect of the latter appears to be negligible, because large mud wave fields at depths greater than 2,400 m (Vorren et al. 1998) indicate that sediments transported through the INBIS channel are deposited much deeper than the high-accumulation area mentioned above.

The various data sets gathered from the study area have been used to validate a numerical model which simulates bottom-arrested turbidity plumes. This simulation includes local topography, grain-size distribution as well as oceanography and demonstrates that particles can be transported to the high-accumulation area and that turbidity plumes can modify the oceanographic environment. Current meter measurements from the Barents Sea and East Greenland continental slopes may provide an idea of time scales of turbidity plumes and how frequently they occur.

Kveitehola – Measurements

For a better understanding of the hydrographic environment in the Kveitehola area quasi-synoptic hydrographic surveys have been carried out. (Blaume 1992; Rumohr et al. this volume). To investigate the processes responsible for high sediment accumulation rates on the continental slope, CTD and transmission measurements with high temporal and spatial resolution have been used to study the regional distribution of water masses and nepheloid layers. Figure 8 shows the regional extent of the BNL above the high-accumulation area. The attenuation at 5 m above the seafloor was more than 50 % higher than in the midwater minimum. The shape and appendix reaching to the Kveitehola Valley indicate that the maximum may come from the shallow Spitsbergen Banken to the northwest. It also suggests that the high-accumulation area may be an export area for resuspended particles. Furthermore, several intrusions of turbid water have been observed at the upper slope in the transition zone between North Atlantic Water (NatW) and Norwegian Sea Deep Water (NwSDW, Fohrmann et al. 1998).

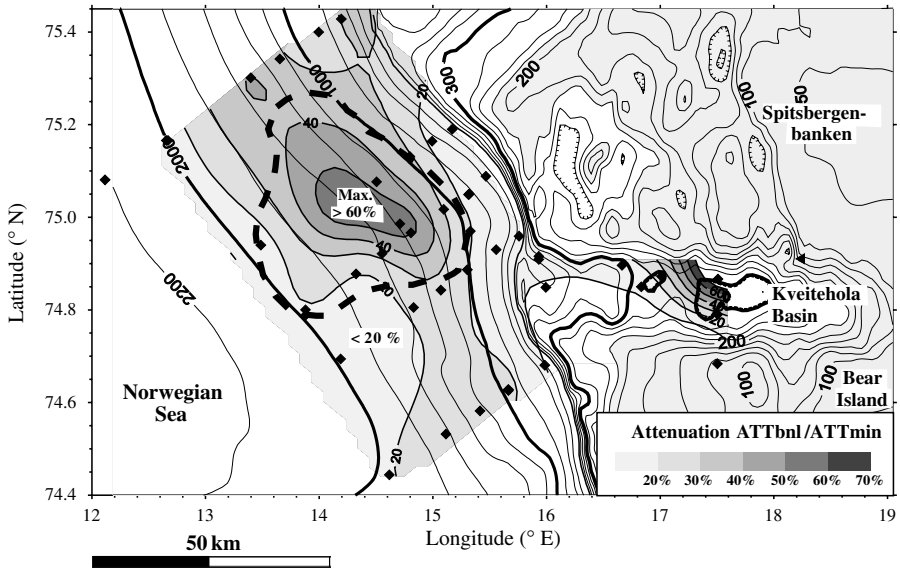

Fig. 8: Correlation of synoptic measurements to geological documentation. Attenuation data were obtained during Poseidon Cruise 181 (March, 1991). Dashed line: the high-accumulation area with Holocene sediments greater than 1 m thick and sediments of Termination I approximately 7 m thick. Gray shading indicates relative attenuation at the bottom normalized by the attenuation minimum in the water column above

Kveitehola – Modeling

To investigate the transport of fine-grained particles from the shallow Spitsbergen Banken to the deep Norwegian Sea, a numerical, hydrostatic, 'reduced-gravity' plume model (Jungclaus et al. 1995) was coupled to an Eulerian sediment transport model (Fohrmann 1996; Fohrmann et al. 1998). The coupled model can take the contribution of suspended sediment to the buoyancy of the plume into account and can simulate erosion, deposition as well as the transport of various grain-size fractions. The grain-size fractions included in the Kveitehola simulation are 20 µm and 63 µm, with settling velocities of 16 m d^{-1} and 165 m d^{-1}. With this model only low-density turbidity plumes can be simulated, therefore a maximal particle concentration (C_{max} = 1 g l^{-1}) is set. The horizontal grid resolution of the model domain is in the order of 250 m. The time interval employed varies between 60 and 600 sec. Variables within the plume are vertically integrated. The ambient water masses are assumed to be at rest, and their temperature and salinity vary vertically. For detailed descriptions of the model see Fohrmann (1996) and Fohrmann et al. (1998).

Figures 9 and 10 show results of a simulation of a turbid plume cascading out of the Kveitehola Valley down the continental slope (Fohrmann et al. 1998). Inflow conditions are described in the figure captions. The plume cascades to a depth of more than 2100 m within 5 days. During the first two days highest plume velocities of up to 1 m s^{-1} occur. The maximal height of the plume is approximately 75 m. After 5 simulation days nearly all particles are deposited and the plume stagnates. The remaining suspended particles ensure that the plume is denser than the ambient water mass. Thus stratification remains stable. If all particles settle out of the suspension, stratification may become unstable, resulting in upward convection (see following section). Figure 10b shows the density contrast between interstitial plume water and ambient water (density as a function of temperature, salinity and pressure only). The light area indicates stable stratification ($\Delta\rho > 0$), the shaded area is unstable ($\Delta\rho < 0$). The net erosion of particles (i.e. the sum of erosion and deposition over the simulation run is negative) occurs mainly on the upper slope (shaded area in Fig. 10a). Net deposition occurs in the high-accumulation area and below at approximately 2100 m. Interestingly, net erosion also occurs in the high-accumulation area, again indicating that the accumulation area may also serve as an export area for resuspended particles. For a shorter inflow period (half a day instead of one day (Fohrmann et al. 1998)) all sediment is deposited within the high-accumulation area. The total volume of the high-accumulation area is V = 1.88 km^{-3}, the deposition rate per year can be calculated to 330 kt a^{-1}. The mean sedi-

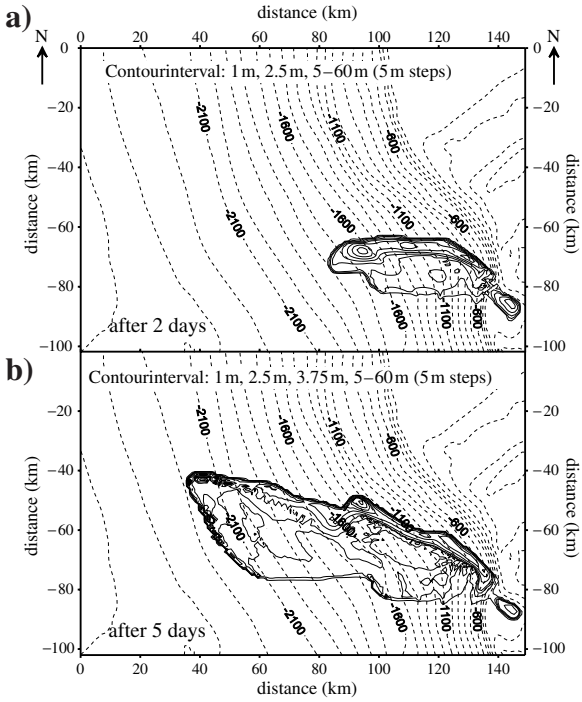

Fig. 9: Kveitehola turbidity plume outflow. The contour plots of plume height (m) at different intervals, after two **(a)** and five **(b)** days of simulation. Inflow stops after one day. Initial sediment concentration is 0.1 g l^{-1} for each particle fraction. Regional bottom sediment availability is 1 mm for 20-µm particles and 0.5 mm for 63-µm particles (Fohrmann et al. 1998)

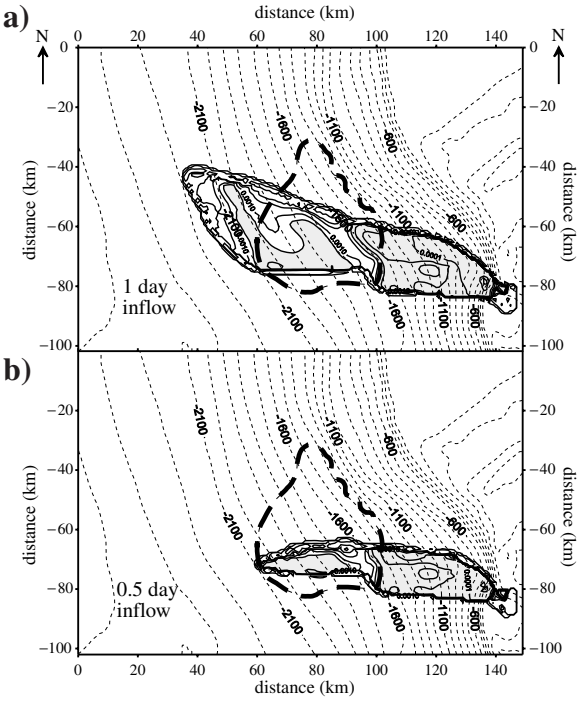

Fig. 10: Contour plots of calculated bottom sediment distribution **(a)** and of density difference between the interstitial water of the plume and the ambient water **(b)** after all particles are deposited. **a)** Areas with net erosion are shaded, whereas areas with net deposition are white, superimposed the high-accumulation area (dashed line); **b)** shaded areas have negative ρ values, white areas are positive (Fohrmann et al. 1998)

mentation rate is on the order of 20 cm ka^{-1} (Blaume 1992; Fohrmann et al. 1998). Based on measurements, numerical results and local topography, the outflow duration at the shelf edge can be estimated to be 2.5 days a^{-1}. Including the numerical results from above, five events lasting half a day are more probable than one event lasting 2.5 days (Fohrmann et al. 1998).

The high-accumulation area observed is located at a depth between 1100 and 2100 m. Other deposition areas, as for example at the INBIS channel farther south, are much deeper (2400 m; Vorren et al. 1998). This may be explained by a channel effect. Flowing in a channel, a turbidite has a smaller interface to the ambient water and therefore entrains less ambient water than a turbidite on a relatively plane continental slope. Consequently, density contrast remains high until the turbidite jumps out of the channel at greater depths.

Convection from Below

Upward convection was investigated with a non-hydrostatic convection model (Kämpf et al. 1997) with a vertical resolution of 10 m. A detailed model description is given in Kämpf (1996) and Kämpf and Backhaus (1998). Without sediments, density stratification (dashed line in Fig. 11) in a 40-m-thick bottom boundary layer is unstable, whereas density stratification with sediment particles is stable (solid line to the right). Upward convection occurs after the deposition of particles if the plume stagnates. The plume becomes thinner (Fig. 11) and ultimately disappears. Less dense water at the top of the plume mixes upward due to small-scale convection, which finally yields to a well-mixed bottom boundary layer. Convection stops after approximately 12 hours, when all particles have settled out. The resulting mixed layer at the bottom is 5.5 times thicker (220 m instead of 40 m) than the initial plume layer. This indicates that characteristics or particles of the plume can be injected far upward into the water column. For stratification weaker than in this simulation, as for example in the Greenland Sea, convection can penetrate much higher than a few hundred meters into the water column. Convection from below penetrating 2000 m into the water columns was, for ex-

ample, observed in the tropical ocean (Quadfasel et al. 1990) or simulated in the laboratory (Kerr 1991). This may explain the observed thicknesses of BBL's in the field, which tend to extend up to several hundred meters above the seafloor.

BI/2 Mooring

From March to July, 1991, a mooring equipped with sediment traps and a current meter 50 m above the seafloor was deployed at a water depth of 2050 m on the continental margin off the western Barents Sea (Thomsen et al. 1998). The position (75°11.87' N, 12°29.21' E) was chosen between potential target areas of bottom-water cascades from the Kveitehola further south or the Storfjordrenna further north. Stick plots of the current meter data (Fig. 12b) show several events (A1–D) with velocities up to 30 cm s^{-1}, which can be related to plumes descending from the shallow shelf area (Fohrmann 1996). Figure 12a shows attenuation and temperature values. During winter, until beginning April, highly frequent variations in attenuation occur with relatively small amplitudes. In spring and summer, variations become more sparse but also stronger. Events A1 and 2 can be considered to be winter events, with low correlation to attenuation and higher correlation to salinity. Attenuation values are generally low in winter because only little sediment is available for erosion and transport. Salinity is elevated during these events, probably because of the release of salt brines on the shelves during ice formation. Spring and summer events B–D, that is, potential turbidity plumes, have higher attenuation values (higher particle load), with the highest values at the beginning, when the plume head carrying most of the particles passes the mooring. Unfortunately, the salinity sensor began to drift to higher values at the beginning of May. Flow directions (Fig. 12b) during the events are parallel to the slope during events A1, A2, C and D. The source area must be somewhere further south, potentially in the Kveitehola Valley or the Bear Island Trough. During the spring event (B), flow is directed perpendicular to the slope, from northeast to southwest. One possible explanation is a plume coming from the Storfjordrenna in the northeast. Again, high salinity values complete the picture of a plume which originates in winter.

EG Mooring

The current meter records presented in Figure 13 show strong bottom intensified episodic currents

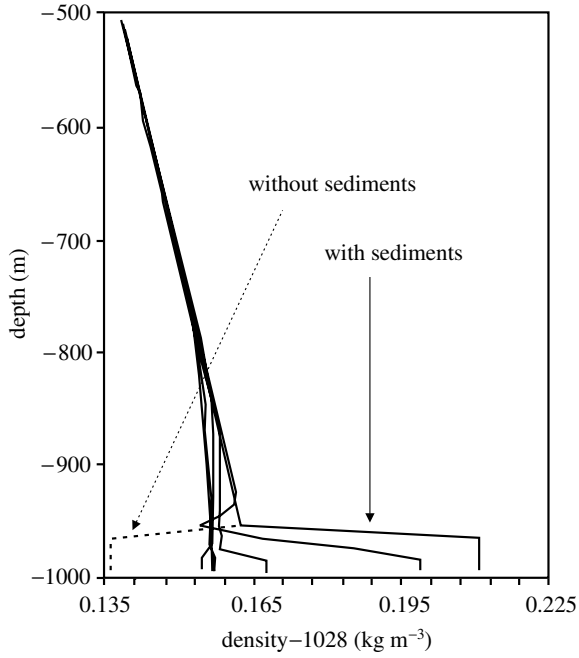

Fig. 11: Evolution of density stratification (solid lines) plotted every third hour of simulation. Dashed line: Initial density stratification without sediments (Kämpf et al. 1997)

(marked A to D) at water depths greater than 3000 m in the Greenland Sea (Woodgate and Fahrbach 1999). Woodgate and Fahrbach describe the events as follows: The current is coherent, but not well-correlated in magnitude, over the entire water column except for event D. The events last from a couple of days up to a week, with changing flow directions. They appear predominantly in the summer season. During the events, the current is modulated by a tidal signal or a signal of frequency close to the Coriolis frequency (f). Correlation to the temperature signal was not observed. The mechanism of these benthic storms is largely unclear. Possibly, the storms are related to turbidity plumes cascading from the East Greenland Shelf. Images of the seafloor, gathered by the deep-towed side-scan sonar system GLORIA (Mienert et al. 1995; Hollender 1996), show channel systems on the continental slope of East Greenland. These V-shaped or U-shaped downslope channels have depths of as much as 120 m, widths of up to 10 km, and are traceable from the shelf edge down to the deep sedimentary basins. Core samples of gravity cores reveal that some of these channels were active after the Last Glacial Maximum (LGM). They may possibly also act as a drainage for turbidity currents and mass flows in modern times.

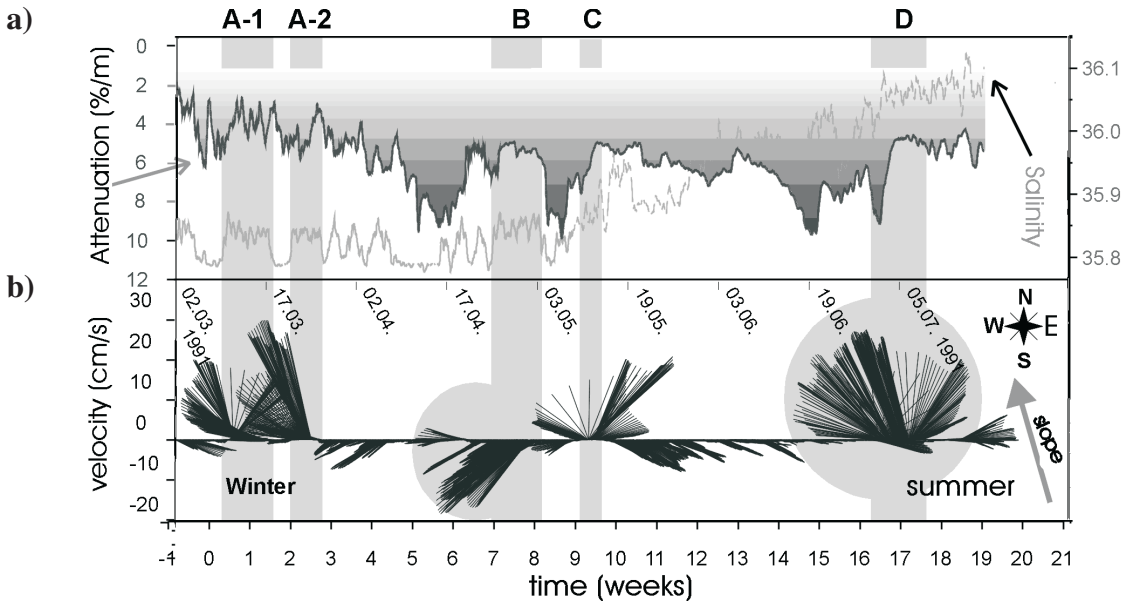

Fig. 12: Attenuation and current velocity at BI Mooring (RCM 7987, Pos.: 75°11.78' N and 12°29.21' E, water depth: 2050 m, instr. depth: 2000 m, Δt = 30 min.). **a)** gray: salinity, black and shaded: attenuation (high values mean high particle load); **b)** current vectors (Fohrmann 1996; Thomsen et al. 1998)

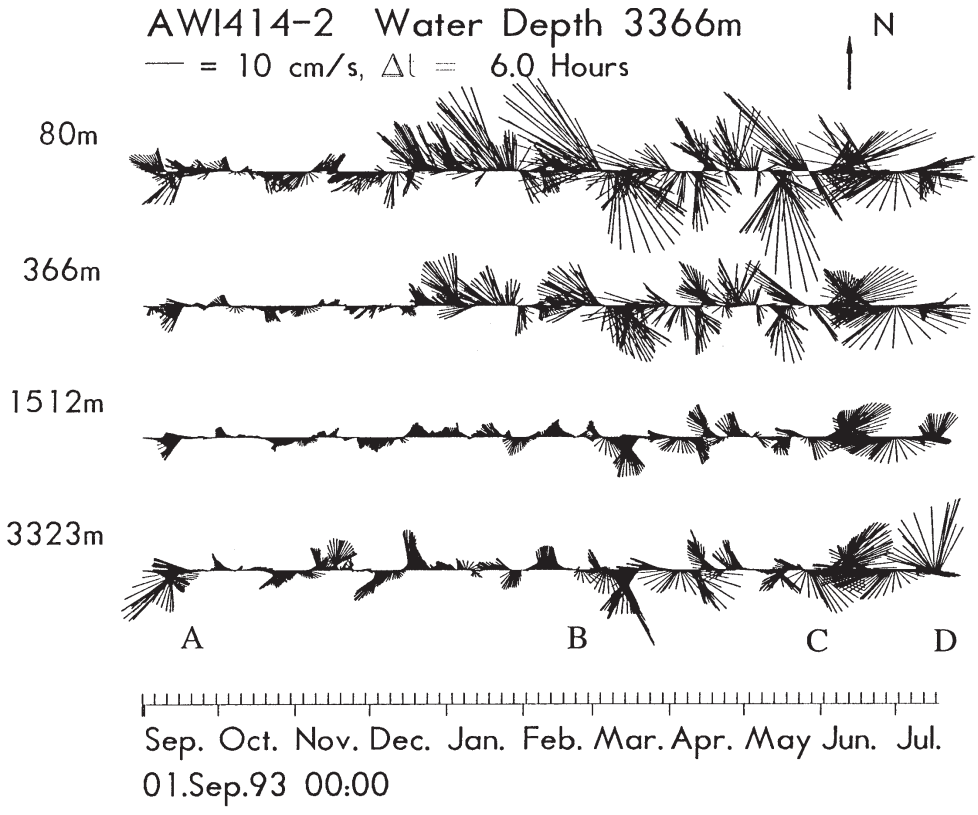

Fig. 13: Stick plots of low-pass filtered data for the four current meters from mooring 414-2. Events are marked A–D (Woodgate and Fahrbach 1999)

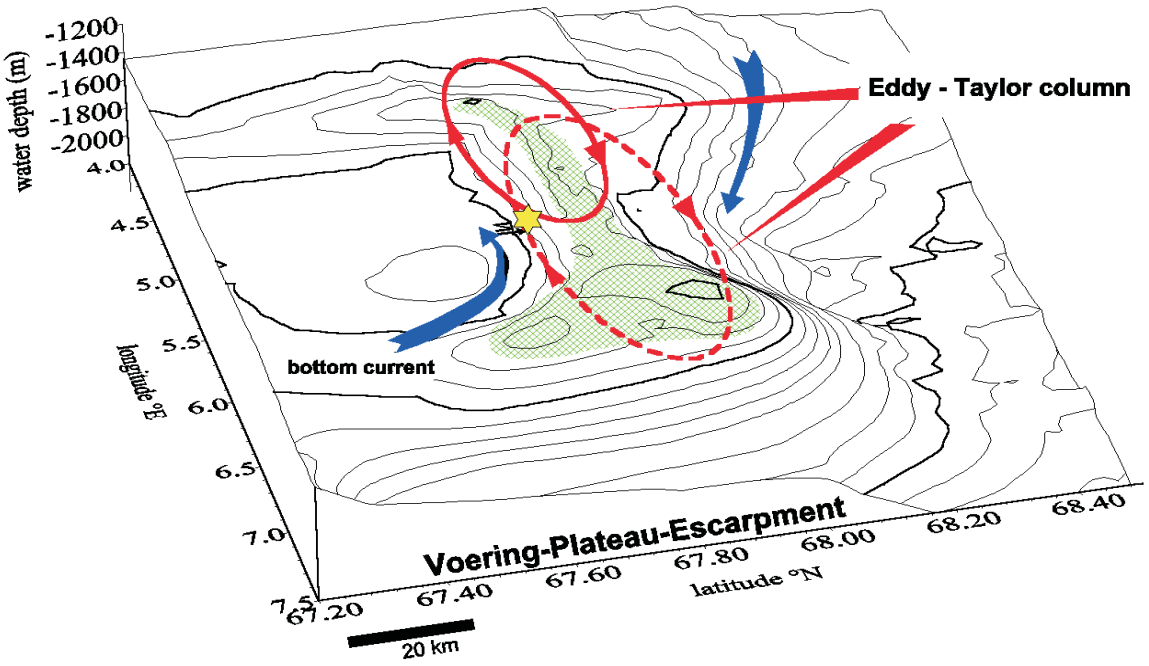

Fig. 14: High-accumulation area on the Vøring Plateau Escarpment. Red circles indicate the position of topographically trapped eddies (Taylor Columns). Green shaded areas indicate the high-accumulation area, blue arrows indicate bottom currents

Taylor Column – Vøring Plateau

At the Vøring Plateau off mid-Norway a high-accumulation area has been observed (Fig. 14) (Rumohr et al. this volume) on the northern slope of the Vøring Plateau Escarpment, a 200-m-high rise at the northern edge of the plateau. Here, accumulation rates are 10 to 30 times higher than at reference stations in close proximity. Current meter measurements and hydrographic surveys suggest that topographically induced eddies control sediment transport and deposition. The source areas of the accumulated sediment can probably be found north of the escarpment, in agreement to simulation results by Schäfer-Neth (1994) and, following Legutke (1989), south of the escarpment. In higher water layers, northward-moving current (Legutke 1989) may induce Taylor Columns with a diameter of 10 to 40 km (Fig. 14). Bottom currents are probably strongly coupled to local topography, at the southern slope of the escarpment mainly to the west, as recorded by current meter measurements. In order to explain the high-frequency oscillations recorded for the current, it may be assumed that, most probably, anticyclonic vortexes move back and forth zonally along the escarpment. Sedimentary material is eroded from the southern slope of the escarpment and deposited in the center of the vortexes on the northern slope (Weber 1995).

Internal Waves – Gamlembanken

The effects imposed by internal waves on particle transport have been investigated in a high-accumulation area on Gamlembanken off mid-Norway. On a transect along 67° N from the continental slope at 8.2° E to the Norwegian Sea at 7.3° E, temperature, salinity, density and attenuation were measured. Following Dickson (1972) and Blaume (1992), Fohrmann (1996) explains the observed doming of the isolines with complex interactions of standing and moving internal waves, as strongly coupled with eddy-like structures within northward-moving North Atlantic Water. Based on density stratification, Figure 15 shows the calculated Brunt-Väisälä-Frequency (a), the inclination of the internal M2-tide (b), and its attenuation on the transect (c). With $f = 2.799 \cdot 10^{-5}$ s^{-1}, the local inertial frequency is lower than the local frequency of the internal M2-tide ($\omega_{M2} = 1.405 \cdot 10^{-4}$ s^{-1}), which yields the first condition for internal M2-tides. The second condition ($\omega_{M2} < N(z)$) is fulfilled for depths less than 900 m. In deeper waters, the Brunt-Väisälä-Frequency may fall below the internal M2-frequency, as indicated by the gray shaded area in Figure 15a. At these depths, internal M2-tides cannot exist. The propagation angle (α) of internal M2-tides is shown in Figure 15b. The small box in Figure 15b shows differences between α and the

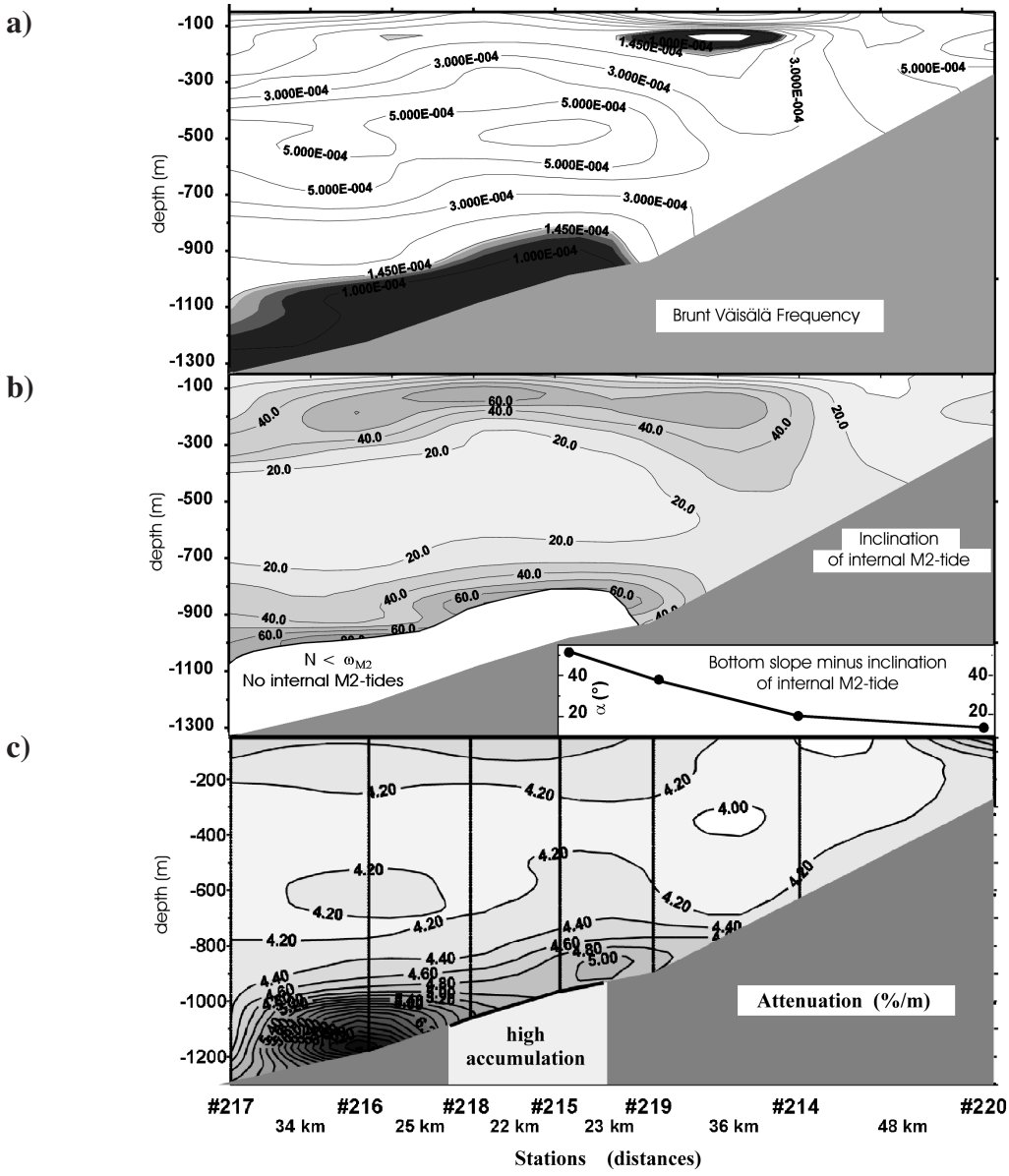

Fig. 15: a) Brunt-Väisälä-Frequency (N) calculated at a transect off mid-Norway (66° N, Gamlembanken–Pos 205). Shaded areas: N < internal M2-tide frequency (w_{M2}); **b)** inclination of internal M2-tide (w_{M2} < N). Lower right corner: Difference between bottom slope and inclination of M2-tide, only where the internal M2-tide reaches the continental slope; **c)** attenuation (% m^{-1}) on the transect off mid-Norway above the high-accumulation area at Gamlembanken

inclination of the slope. This difference decreases from 40° at 900 m depth to 10° at 400 m. As described above, the smaller the angle is, the larger the energy transfer along the seafloor becomes. This means highest erosion by strong bottom currents induced by internal M2 surf may occur close to the shelf edge. Here, reflected internal waves may travel down to a depth of approximately 900 m, where they may be reflected seaward. Eroded particles may be transported downslope by internal tidal currents close to the seafloor and deposited below 900 m water depth, where no internal waves can occur (Fig. 15c).

BNL–Modeling

The distance to which the particles may be transported after being released into the water mass depends on flow velocity and the turbulence of the current. The res-

idence time of a particle in the water column is directly related to its settling velocity. The faster a particle settles, the shorter the residence time and, in turn, its transport distance is. Very rapidly sinking particles, with settling velocities of up to 200 m d^{-1}, settle in approximately 15 days to 3000 m depth. In this time, a mean current of 5 cm s^{-1} will transport the particles horizontally over approximately 65 km. Slowly sinking particles with a settling velocity of approximately 10 m d^{-1} can be transported horizontally over distances of more than 1300 km. Suspended particles with settling velocities close to zero remain in suspension and travel much further (Haupt et al. 1998), as shown in Figure 2. In a water column, interacting particles may aggregate and form particles with higher settling velocities (Stolzenbach 1993). Due to strong current shear near the seafloor particle interactions in the BBL are more complex. These interactions lead to hydrodynamic sorting as described above. A one-dimensional advection-diffusion model has been developed to study particle interactions in the BBL (Ritzrau and Fohrmann 1998). This model has a high vertical resolution, with Δz increasing exponentially from 1 mm at the seafloor to approximately 1000 m in the uppermost layer. This includes vertical particle advection (particle settling), vertical diffusion (turbulence) as well as particle interactions, such as turbulent aggregation, differential settling and disaggregation. The three particle classes used in the model are defined by particle diameter and settling velocity. Aggregates larger than the largest particle class are transferred to a particle sink. The concentration distribution of suspended particles simulated at steady state (after approximately one simulation day) is shown in Figure 16a. Particle concentration increases strongly towards the seafloor, exceeding 1 g l^{-1} in the last few centimeters. Close to the seafloor, the most rapidly sinking particle class has highest concentrations. At 10 centimeters and more above the seafloor the smallest, and thus slowest, particles dominate. Hydrodynamic sorting is more obvious in Figures 16b and c, showing the fraction of total mass for each particle class for a model run without particle interactions. In both hydrodynamic regimes, rapidly sinking particles dominate close to the seafloor and slow sinking particles in the water mass above. For the low-velocity regime, particles are transported up to 30 m height, in the high velocity regime to more than 120 m height above the seafloor. Particle size distribution in the BBL is significantly altered after particle interactions are introduced (Figs. 16d and e). In both hydrodynamic regimes nearly all slow sinking particles are absent (as aggregates they have moved to larger classes); only a small fraction still remains in the low-velocity regime. For the low-velocity regime, hydrodynamic sorting occurs comparable to the runs without particle interaction (Fig. 16b). For the high velocity regime the more rapidly sinking particle classes are spread nearly homogeneously over the BBL, with a clear dominance of the most rapid and largest particle class. Further studies with more than three particle classes (not shown here) suggest that larger particles, that is, larger than the particles in the study presented here, will be destroyed and transported upward again, due to current shear. The simulation illustrates that hydrodynamic sorting and particle interactions due to current shear in the BBL remove the finest particles and produce a vertical particle composition with largest particles in close vicinity to the seafloor and finer particles distributed nearly homogeneously in the upper BBL.

Sediment Transport in a Paleoenvironment

A similar attempt to investigate the 'Paleo-Greenland-Iceland-Norwegian Seas' on a process-based approach was undertaken by Michels (1995). Based on high-resolution settling velocity analyses of 120 sediment surface samples and nine cores on two transects at latitudes of 68 to 70° N and 76 to 77° N in the Greenland-Iceland-Norwegian Seas, current transported sediment fractions were identified and critical shear velocities and maximum geostrophic current velocities for their transport were reconstructed.

The resulting pattern of reconstructed current velocities from 120 sediment surface samples in the Norwegian-Greenland Seas reflects the known oceanographic features of present-day thermohaline circulation, which is influenced by topography in many places.

In general, the distribution of reconstructed maximum geostrophic current velocities shows a large-scale increase of current velocity from the southwest to the northeast and a dependence of current velocity on water depth, the restriction of the flow path by topographic barriers and focusing of geostrophic currents, particularly along the Greenland continental slope. The sorting characteristics of the sediment samples, well-sorted, residual and low-energy depositional, give some indication of the processes which prevailed during deposition of the sediments.

Residual sediments occur on the Spitsbergen Bank, in the Fram Strait and in the central Greenland Basin. Well-sorted sediments are common in the Fram Strait (Eiken and Hinz 1993) and the Greenland Basin, but

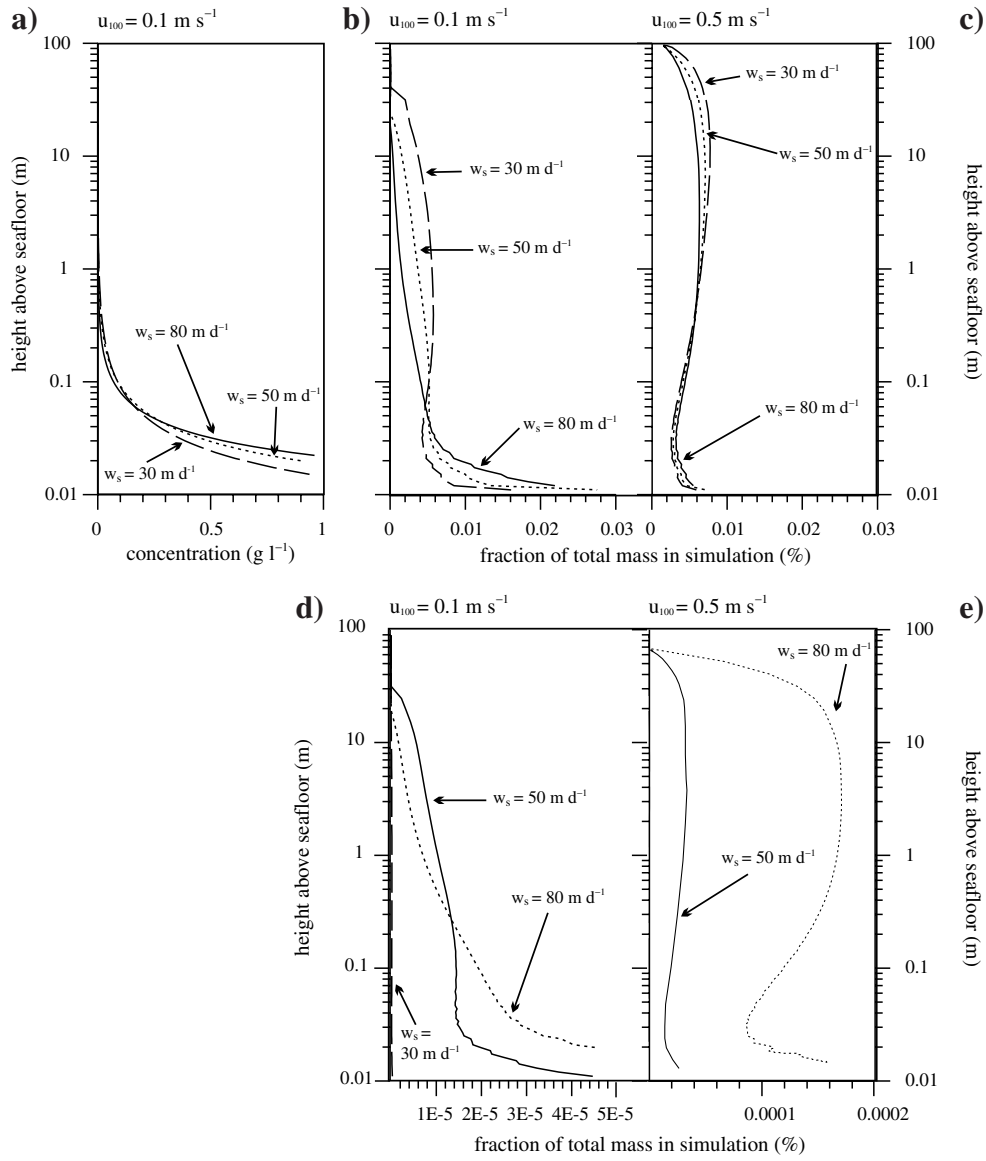

Fig. 16: a) Concentration of suspended particles for rapidly sinking particles (solid line: w_s = 80 m d^{-1}), slowly sinking particles (dashed line: w_s = 30 m d^{-1}), and other particles with w_s = 50 m d^{-1} (dotted line); **b–e)** fraction of total suspended mass for the particles classes (described for Fig. 16a) for various hydrodynamic regimes; **b)** and **c)** diffusion advection alone; **d)** and **e)** particle interactions incl; **b)** and **d)** calm (u_{100} = 0.1 m s^{-1}); **c)** and **e)** rough (u_{100} = 0.5 m s^{-1})

also on the Vøring Plateau. Large areas on the Iceland Plateau, in the Norway and Lofoten Basins and over the central part of the Old Jan Mayen Fracture Zone, as well as on the Greenland continental slope, are characterized by low-energy depositional sediments. These results indicate that the Fram Strait, the western Greenland Basin and the Greenland continental slope are characterized by strong contourite currents which cause a widespread sorting of sediments with the occasional occurrence of residual sediments (Eiken and Hinz 1993). Gravitational transport on the continental slopes probably contributes to the sorting of sediments as well. The application of this method to nine cores gives an indication of the changes in oceanographic and sedimentologic conditions during Oxygen Isotope Stages 6, 5, 2 and 1. These changes can be characterized as follows.

In Oxygen Isotope Stages 6 and 2, gravitational downslope transport of sediment dominated on the Norwegian continental shelf as a result of high accu-

mulation rates of terrigenous material and an intensified generation of dense bottom waters on the shelves (Holtedahl and Bjerkli 1975; Damuth 1978; Rasmussen 1984; Thiede et al. 1986). In contrast, the sedimentary regime in Stages 5 and 1 was characterized by geostrophic currents in these regions (Sejrup et al. 1984; Henrich 1986). On the Iceland Plateau, the differences between the glacial and interglacial sedimentary regimes are less pronounced.

Turbiditic sediments prevail in the area of the Greenland Fracture Zone in glacial and perhaps in interglacial times (Eiken and Hinz 1993); they are interbedded with contouritic sediments during the climatic optima in Substage 5.5 and in the Holocene.

Discussion

The large- and small-scale modern ocean current controlled sediment transport processes presented here reveal a complex 'particle conveyer belt' from shallow areas or surface layers to deep basins or adjacent oceans. Consequently, any attempt to calculate a particle budget must be as complicated as the processes involved.

The large-scale simulations described above indicate that the northern North Atlantic must be seen as a source or sink of particles for the world oceans. Across the northern cross-sections, 3.31 Mio t a^{-1} of sediment are exported to the Arctic Ocean (Fig. 3), whereas 2.12 Mio t a^{-1} are imported from the North Atlantic Ocean, across the straits between Greenland and Norway. For the northern North Atlantic this gives a net particle export of approximately 1.19 Mio t a^{-1} to the north. Because of unknown errors in topography and sediment supply and the absence of small-scale processes in the large-scale model, this number may only be used for a rough budgeting estimate. Nevertheless it demonstrates that the northern North Atlantic cannot be treated as a closed basin.

So far, investigations of small-scale processes may also not be used to calculate numbers for a particle transport budget, but insights into these processes can be used to divide the northern North Atlantic into various areas in which different processes predominate. In those areas differing transport and sedimentation rates may be expected.

The depth range between the shelf break at approximately 500 m water depth and the 1000 m isobath (dark gray in Fig. 17), extending as a very narrow band along the entire boundaries of the northern North Atlantic, can be seen as a potential area for the erosion of surface sediments. Here, internal waves may reach the continental slope and start erosion, for example as an additional process to winnowing. Deeper, between 1000 and 2000 m water depth (light gray in Fig. 17), the seafloor is influenced by deep contour currents. Two regional exceptions, the Vøring Plateau and the Iceland Plateau, are obvious. The first shows, due to eddy-seafloor interactions, different sedimentation patterns, and is well known for its exceptional characteristics for various biological and chemical parameters (see Ritzrau et al. this volume and Schlüter et al. this volume). The second is a larger and shallower plateau, compared to the deeper basins. Therefore it must be treated differently (Ritzrau et al. this volume).

The decisive parameter for downslope particle transport is the inclination of the seafloor. Steep slopes ($\alpha > 0.5°$ diagonal hatching in Fig. 17) occur on continental slopes just below the shelf break in the entire northern North Atlantic. On the eastern side these steep slopes extend down to approximately 2000 m water depth, on the western side they are much deeper (approximately 3000 m). Steep slopes also occur at the edge of the Island Plateau and along the ridges between the Greenland Basin and the Lofoten Basin and further north. These areas can be seen as erosion or transit regions through which downslope currents pass on their way to the deeper basins. All these slope-defined areas must be calculated differently because of the differing sediment supply, which is probably largest at the Barents Shelf. If smoother slopes ($0.25° < \alpha < 0.5°$) are added to the transit areas, only a small part of the deep basins can be treated as deposition areas. The largest can be found in the Lofoten Basin (white areas in Fig. 17).

Sediment import from the shallow shelves strongly depends on the renewal of sediment sources. Sediment import from the Barents Shelf or the Norwegian Shelf is relatively well known. Here renewal is dominated by sea ice-transported particles, the production of carbonate sands on shallow banks, and by glacial sediment supply. On the Greenland side information is rare, but sediment delivery by glaciers and sea ice transport from the Arctic Ocean into the Greenland Sea plays an important role.

Additionally, some areas have exceptional characteristics. For example, the Vøring Plateau, as mentioned above, or the NE water Polynya area at the western side of Fram Strait. The latter is influenced by a partly sea ice-free polynya and a relatively stable small-scale eddy-like recirculation structure which inhibits particle export from the polynya to the East Greenland Current (Ritzrau and Thomsen 1997).

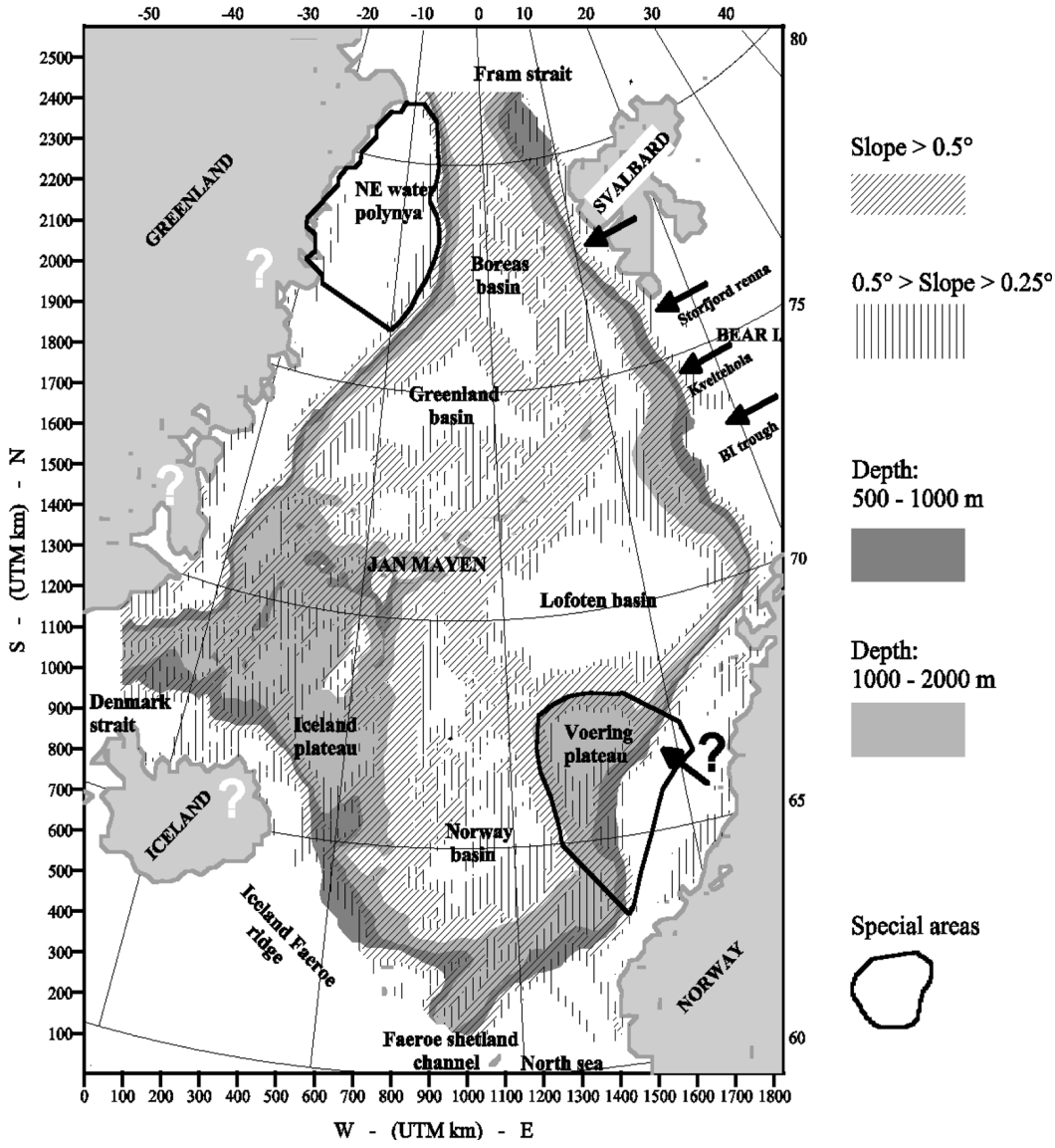

Fig. 17: The northern North Atlantic divided in various areas with respect to the particular dominating sediment transport processes. See legend for explanations. Black arrows indicate known areas in which sediments are transported from the shallow shelf to the deep basins. Question marks indicate uncertainties about terrigenous sediment supply

By identifying critical shear velocities and maximum geostrophic current velocities, investigations of current transported sediment fractions reflect the modern oceanographic features of large-scale circulation. Therefore, this method is useful for assessing large-scale circulation patterns for paleoenvironments if the regional distribution of sediment cores used is high. However, small-scale processes can only be outlined roughly and must be assessed based on investigations of processes in the modern environment.

Conclusions

Modern ocean current controlled particle transport in the northern North Atlantic is strongly coupled to the large-scale circulation regime, which results in sediment transfer across the large openings in the north and south. The geostrophic component of particle transport can be simulated and roughly estimated using a large-scale circulation model. Small-scale processes may, however, substantially alter large-scale sediment transport and change sedimentation rates. These small-scale

processes have been carefully studied (both in the field and by numerical modeling) at several locations in the northern North Atlantic. The cascading of dense water masses from shallow shelves, as observed at the Barents Shelf (BI mooring) or the East Greenland Shelf (EG mooring), is an important process for transporting particles from the slope into deep-ocean basins. The settling of these deep-flowing particles may be strongly affected by contour bottom currents, convection from below, and particle interaction. Particles may escape settling near the slope and may be transported far away by large-scale circulation. At water depths between 500 and 1000 m, internal waves may reach the continental slopes and mobilize sediments at the seafloor, which may be further transported in the BBL, or as cascading plumes. Suspended particles may be trapped by eddies at rises in the seafloor (Vøring Plateau).

The results of this study have been used to divide the northern North Atlantic into several separated areas with distinctly different sedimentation processes. This type of regional division is similar to methods used in addressing the carbon budget on the areal distinction basis (Ritzrau et al. this volume and Schlüter et al. this volume).

Particle transport in the northern North Atlantic is a highly complex interaction of large- and small-scale sediment transport processes. A detailed description of the processes involved at selected locations has been presented schematically and on the basis of field data and numerical simulations. To draw a realistic picture for the entire northern North Atlantic a regionally much more highly resolved data base must be developed to examine the strength of the processes involved at representative locations.

Acknowledgments

The authors thank the crews of RV's Poseidon, Valdivia, and Meteor for their assistance during cruises. Maren Hein and Christine Voigt, as well as those who collaborated with them, are thanked for superb laboratory work. We appreciate the professional assistance of Helmut Beese and Erik Steen before and during our field work. We acknowledge the support of and many fruitful discussions with colleagues at the SFB 313, the Alfred Wegener Institute, the Institute for Marine Science Hamburg, and GEOMAR. Last, but not least, we thank T.O. Vorren, J.S. Laberg, R.W. Sternberg and E. McPhee for their critical and helpful reviews.

This study was funded by the German Science Foundation.

References

Aagaard, K., J. H. Swift, and E. C. Carmack, Thermohaline circulation in the Arctic mediterranean seas, *J. Geophys. Res.*, 90 (C3), 4833–4846, 1985.

Aagaard, K., A synthesis of the Arctic Ocean circulation, *Rap. P.-v. reun. Int. Explor. Mer*, 188, 11–22, 1989.

Alldredge, A. L., and M. W. Silver, Characteristics, dynamics and significance of marine snow, *Prog. Oceanogr.*, 20, 41–82, 1988.

Backhaus, J. O., H. Fohrmann, J. Kämpf, and A. Rubino, Formation and Export of water masses produced in Arctic shelf polynyas, process studies on oceanic convection, *ICES Journal of Marine Sciences*, 54 (3), 366–382, 1997.

Berner, R. A., Burial of organic carbon and pyrite sulfur in the modern ocean: Its geochemical and environmental significance, *Am. J. Sci.*, 282, 451–473, 1982.

Blaume, F., Hochakkumulationsgebiete am norwegischen Kontinentalhang: Sedimentologische Abbilder topographiegeführter Strömungsmuster, *Ber. SFB 313, Univ. Kiel*, 36, 170 pp., 1992.

Bryan, K., A numerical method for the study of the circulation of the world ocean, *J. Comput. Phys.*, 4, 347–376, 1969.

Cox, M. D., A primitive equation, 3-dimensional model of the ocean, *GFDL Ocean Group Technical Report No. 1*, 250 pp., Princeton N.J., 1984.

Damuth, J. E., Echo character of the Norwegian-Greenland Sea: relationship to Quaternary sedimentation, *Mar. Geol.*, 28, 1–36, 1978.

Dickson, R. R., Variability and continuity within the Atlantic current of the Norwegian Sea, *Rap. P.-v. reun. Int. Explor. Mer*, 162, 167–183, 1972.

Eiken, O., and K. Hinz, Contourites in the Fram Strait, *Sedimentary Geology*, 82, 15–32, 1993.

Elverhøi, A., and A. Solheim, The physical environment of the western Barents Sea, 1:1,500,000 Sheet A: Surface sediment distribution, *Norsk Polarinstitutt Skrifter*, 179, 3–14, 1983.

Fahrbach, E., and J. Meincke, High-frequency velocity fluctuations on a steep continental slope, *Rap. P.-v. reun. Int. Explor. Mer*, 180, 76–77, 1982.

Fohrmann, H., Sedimente in bodengebundenen Dichteströmungen – numerische Fallstudien, *Ber. SFB 313, Univ. Kiel*, 66, 106 pp., 1996.

Fohrmann, H., J. O. Backhaus, F. Blaume, and J. Rumohr, Sediments in bottom arrested gravity plumes – numerical case studies, *J. Phys. Oceanogr.*, 28 (11), 2250–2274, 1998.

Haupt, B. J., C. Schäfer-Neth, and K. Stattegger, Modeling sediment drifts: A coupled oceanic circulation-sedimentation model of the northern North Atlantic, *Paleoceanography*, 9, 897–916, 1994.

Haupt, B. J., D. Seidov, and K. Stattegger, SEDLOB and PATLOB: Two numerical tools for modeling climatically-forced sediment and water volume transport in large ocean basins, in *Modeling of Sedimentary Systems*, edited by J. Harff, W. Lemke, and K. Stattegger, 33 pp., Springer, Heidelberg, 1998.

Henrich, R., A calcite dissolution pulse in the Norwegian-Greenland-Sea during the last deglaciation, *Geol. Rundsch.*, 75, 805–827, 1986.

Holtedahl, H., and K. Bjerkli, Late Quaternary sediments and stratigraphy on the continental shelf off More-Trondelag, W. Norway, *Mar. Geol.*, 45, 179–226, 1982.

Huthnance, J. M., Circulation, exchange and water masses at the ocean margin: the role of physical processes at the shelf edge, *Prog. Oceanogr.*, 35, 353–431, 1995.

Hollender, F. - J., Untersuchung des ostgrönländischen Kontinentalrandes mit dem Weitwinkel-Seitensicht-Sonar GLORIA, *Ber. SFB 313, Univ. Kiel*, 67, 124 pp., 1996.

Hopkins, T. S., The Gin Sea Review of physical oceanography and literature from 1972, *Saclantcen Report*, Saclant Undersea Research Center, San Bartolomeo, Italy, Ser.nr.: SR-124, 195 pp., 1988.

Jungclaus, J. H., J. O. Backhaus, and H. Fohrmann, Outflow of dense water from the Storfjord in Svalbard: A numerical model study, *J. Geophys. Res.*, 100 (C12), 24719–24728, 1995.

Kämpf, J., Thermohaline Konvektion in Polynien arktischer Schelfmeere, *Report of the Center of Marine and Climate Research*, *University Hamburg*, 23, 192 pp., 1996.

Kämpf, J., H. Fohrmann, and J. O. Backhaus, On the potential role of sediments in Arctic slope-convection, *Proceedings of the conference on Polar Processes and Global Climate*, Rosario, Orcas Island, USA, 3 pp., 1997.

Kämpf, J., and J. O. Backhaus, Shallow, brine-driven free convection in polar oceans: nonhydrostatic numerical process studies, *J. Geophys. Res.*, 103, 5577–5593, 1998.

Kenyon, N. H., Evidence from bedforms for a strong poleward current along the upper continental slope of northwest Europe, *Mar. Geol.*, 72, 187–198, 1986.

Kerr, R. C., Erosion of stable density gradient by sediment-driven convection, *Nature*, 353, 423–425, 1991.

Killworth, P., Deep convection in the world ocean, *Rev. Geophys. Space Physics*, 21, 1–26, 1983.

Laberg, J. S., and T. O. Vorren, Late Weichselian submarine debris flow deposits on the Bear Island Trough Mouth Fan, *Mar. Geol.*, 127, 45–72, 1995.

LeBlond, P. H., and L. A. Mysak, Waves in the Ocean, 602 pp., Elsevier Oceanography, New York, 1978.

Legutke, S., Modelluntersuchungen zur Variabilität im Strömungsmuster des Europäischen Nordmeeres, *Report of the Center of Marine- and Climate Research*, *University Hamburg*, 4, 209 pp., 1989.

Mienert, J., F. - J. Hollender, and N. H. Kenyon, GLORIA survey of the East Greenland margins: 70° N to 80° N, in *Sea Floor Atlas of the Northern Norwegian-Greenland Sea*, edited by K. Crane, and A. Solheim, 172 pp., Norsk Polarinstitutt, Milasotampa S.p.A. Italy, Knut Hässlers Bokbinderi, Sweden, 1995.

Michels, K., The decomposition of polymodal settling velocity distributions for a comprehensive sedimentological description of sand-sized samples, *Sedimentology*, 42, 31–38, 1995.

McCave, I. N., Size spectra and aggregation of suspended particles in the deep ocean, *Deep-Sea Res.*, 31, 329–352, 1984.

Munk, W., Internal Waves and Small-Scale Processes, in *Evolution of Physical Oceanography*, edited by B. A. Warren, and C. Wunsch, pp. 264–291, MIT Press, Massachusetts, 1981.

Pacanowski, R., K. Dixon, and A. Rosati, The GFDL Modular Ocean Users Guide, *GFDL Ocean Group Technical Report No. 2*, GFDL/NOAA, Princeton University, 1993.

Pedlovsky, J., *Geophysical Fluid Dynamics*, 706 pp., Springer, New York, 1987.

Pfirman, S. L., Modern sedimentation in the northern Barents Sea: Input, dispersal, and deposition of suspended sediment from glacial meltwater, *Mass. Inst. Tech./Woods Hole Oceanogr. Inst., Tech. Rep. WHOI-85-4*, 382, 1985.

Poulain, P. - M., A. Warn-Varnas, and P. P. Niiler, Near surface circulation of the Nordic Seas as measured by Lagrangian Drifters, *J. Geophys. Res.*, 101 (C8), 18237–18258, 1996.

Quadfasel, D., H. Kudrass, and A. Frische, Deep water renewal by turbidity currents in the Sulu Sea, *Nature*, 348, 320–322, 1988.

Quadfasel, D., B. Rudels, and K. Kurz, Outflow of dense water from a Svalbard fjord into the Fram Strait, *Deep-Sea Res.*, 35 (7), 1143–1150, 1990.

Rasmussen, A., Late Weichselian moraine chronology of the Vesterålen islands, North Norway, *Nor. Geol. Tidsskr.*, 64, 193–219, 1984.

Ritzrau, W., and L. Thomsen, Spatial distribution of particle composition and microbial activity in benthic boundary layer (BBL) of the Northeast Water Polynya, *Journal of Marine Science*, 10, 415–428, 1997.

Ritzrau, W., and H. Fohrmann, Field and numerical studies of near bed aggregate dynamics, in *Computerized Modeling of Sedimentary Systems*, edited by J. Harff, W. Lemke, and K. Stattegger, pp. 183–207, Springer, Heidelberg, 1998.

Ritzrau, W., G. Graf, A. Scheltz, and W. Queisser, Bentho-pelagic coupling and carbon dynamics in the northern North Atlantic, this volume.

Rudels, B., and D. Quadfasel, Convection and deep water formation in the Arctic Ocean-Greenland Sea system, *J. Mar. Syst.*, 2, 435–450, 1991.

Rumohr, J., F. Blaume, H. Erlenkeuser, H. Fohrmann, F. - J. Hollender, J. Mienert, and C. Schäfer-Neth, Records and processes of near-bottom sediment transport along the Norwegian-Greenland Sea margins during Holocene and Late Weichselian (Termination I) times, this volume.

Ross, J., *Modellexperimente zur topographischen Deformation einer ebenen Strömung*, Diploma thesis, University Hamburg, 57 pp., 1991.

Schäfer, P., J. Thiede, S. Gerlach, G. Graf, E. Suess, and B. Zeitzschel, The environment of the northern North-Atlantic Ocean: Modern depositional processes and their historical documentation, this volume.

Schäfer-Neth, C., Modellierung der Paläoozeanographie des nördlichen Nordatlantiks zur letzten Maximalvereisung, *Ber. SFB 313, Univ. Kiel*, 51, 105 pp., 1994.

Schauer, U., The release of brine-enriched shelf water from the Storfjord into the Norwegian Sea, *J. Geophys. Res.*, 100 (C8), 16015–16028, 1995.

Schlüter, M., E. J. Sauter, D. Schulz-Bull, W. Balzer, and E. Suess, Fluxes of organic carbon and biogenic silica reaching the seafloor: A comparison of high northern and southern latitudes of the Atlantic Ocean, this volume.

Seidov, D., Numerical modeling of the ocean circulation and paleocirculation, Mesozoic and Cenozoic oceans, *Geodyn. Ser.*, 15, edited by K. J. Hsu, pp. 11–26, AGU, Washington, D.C., 1986.

Seidov, D., An intermediate model for large-scale ocean circulation studies, *Dyn. Atmos. Oceans*, 25 / 1, 25–55, 1996.

Seidov, D., and B. J. Haupt, Simulated ocean circulation and sediment transport in the North Atlantic during the last glacial maximum and today, *Paleoceanography*, 12, 281–305, 1997a.

Seidov, D., and B. J. Haupt, Global ocean thermohaline conveyor at present and in the late Quaternary, *Geophys. Res. Lett.*, 24, 2817–2820, 1997b.

Sejrup, H. P., E. Jansen, H. Erlenkeuser, and H. Holtedahl, New faunal and isotopic evidence on the Late Weichselian-Holocene oceanographic changes in the Norwegian Sea, *Quat. Res.*, 21, 74–84, 1984.

Stolzenbach, K. D., Scavenging of small particles by fast sinking porous aggregates, *Deep-Sea Res.*, 40, 359–369, 1993.

Thiede, J., G. W. Diesen, B. - E. Knudsen, and T. Snåre, Patterns of Cenozoic sedimentation in the Norwegian-Greenland Sea, *Mar. Geol.*, 69, 323–352, 1986.

Thomsen, C., F. Blaume, H. Fohrmann, J. Maaßen, I. Peeken, and U. Zeller, Particle transport processes at slope environments – event driven flux across the Barents Sea continental margin, submitted to *Mar. Geol.*, 1998.

Thorpe, S. A., and M. White, A deep intermediate nepheloid layer, *Deep-Sea Res.*, 35 (9), 1665–1671, 1988.

Vogt, P. R., Seafloor Topography, Sediments, and Paleoenvironments, in *The Nordic Seas*, edited by B. G. Hurdle, pp. 237–412, Springer, Heidelberg, 1986.

Vorren, T. O., J. S. Laberg, F. Blaume, J. A. Dodeswell, N. H. Kenyon, J. Mienert, J. Rumohr, and F. Werner, The Norwegian Greenland Sea Continental Margins: Morphology and Late Quaternary Sedimentary Processes and Environment, *Quat. Sci. Rev.*, 17, 273–302, 1998.

Weber, M., Sedimentologische Untersuchungen eines Holozänen Hochakkumulationsgebietes auf dem Vøring Plateau Escarpment (Norwegische See) zur Frage des Sedimenttransportes in der Tiefsee, Diploma thesis, *SFB 313, Univ. Kiel*, 1995.

Woodgate, R. A, and E. Fahrbach, Benthic Storms in the Greenland Sea, *Deep-Sea Res.* 46, 2109–2127, 1999.